HHS Public Access

Author manuscript

*Nat Mater*. Author manuscript; available in PMC 2013 March 03.

Published in final edited form as:

*Nat Mater*. 2012 September ; 11(9): 768–774. doi:10.1038/nmat3357.

# Rapid casting of patterned vascular networks for perfusable engineered 3D tissues

**Jordan S. Miller**[a], **Kelly R. Stevens**[b], **Michael T. Yang**[a], **Brendon M. Baker**[a], **Duc-Huy T. Nguyen**[a], **Daniel M. Cohen**[a], **Esteban Toro**[a], **Alice A. Chen**[b], **Peter A. Galie**[a], **Xiang Yu**[a], **Ritika Chaturvedi**[a], **Sangeeta N. Bhatia**[b,c,d], and **Christopher S. Chen**[a,e]

[a]Department of Bioengineering, University of Pennsylvania, Philadelphia, PA 19104

[b]Harvard-MIT Division of Health Sciences and Technology, Massachusetts Institute of Technology, Cambridge, MA 02139

[c]Howard Hughes Medical Institute, Cambridge, MA 02139

[d]Department of Electrical Engineering and Computer Science, Massachusetts Institute of Technology, Cambridge, MA 02139

## Abstract

In the absence of perfusable vascular networks, three-dimensional (3D) engineered tissues densely populated with cells quickly develop a necrotic core [1]. Yet the lack of a general approach to rapidly construct such networks remains a major challenge for 3D tissue culture [2–4]. Here, we 3D printed rigid filament networks of carbohydrate glass, and used them as a cytocompatible sacrificial template in engineered tissues containing living cells to generate cylindrical networks which could be lined with endothelial cells and perfused with blood under high-pressure pulsatile flow. Because this simple vascular casting approach allows independent control of network geometry, endothelialization, and extravascular tissue, it is compatible with a wide variety of cell types, synthetic and natural extracellular matrices (ECMs), and crosslinking strategies. We also demonstrated that the perfused vascular channels sustained the metabolic function of primary rat hepatocytes in engineered tissue constructs that otherwise exhibited suppressed function in their core.

---

Living tissues have complex mass transport requirements that are principally met by blood flow through multiscale vascular networks of the cardiovascular system. Such vessels deliver nutrients and oxygen to, and remove metabolic byproducts from, all of the organ systems in the body and were critical to the rise of large-scale multicellular organisms [5]. Although tremendous progress has been made in the past several decades to isolate and culture cells from native tissues, simple methods to generate tissue constructs populated at

---



[e]To whom correspondence should be addressed. chrischen@seas.upenn.edu.

**Author Contributions**

J.S.M. and C.S.C. conceived and initiated the project. J.S.M., K.R.S., M.T.Y., B.M.B., D-H.T.N., D.M.C., E.T., A.A.C., P.A.G., X.Y., and R.C. designed and performed experiments. C.S.C. and S.N.B. supervised the project.

physiologic cell densities that are sustained by even the most basic vascular architectures have remained elusive.

To create perfusable channels in engineered tissues, layer-by-layer assembly [6–9] has been explored. In this approach, a trench is molded into one layer such that a second, separately fabricated layer can then be aligned and laminated to close the lid to form channels in an iterative fashion. However, layer-by-layer assembly is slow and results in seams or other structural artifacts throughout the construct while simultaneously placing considerable design constraints on the materials, channels, and cells used during fabrication. Bioprinting [10], in which cells and matrix are deposited dropwise, has been developed over the past decade but also is a slow, serial process with limitations on print resolution, materials, and cells. In contrast to these methods, 3D sacrificial molding [11–13] provides an intriguing alternative. Proof-of-concept studies have shown that a network of channels can be fabricated by creating a rigid 3D lattice of filaments, casting the lattice into a rubber or plastic material, and then sacrificing the lattice to reveal a microfluidic architecture in the bulk material. However, 3D sacrificial molding of perfusable channels has so far required the use of cytotoxic organic solvents or processing conditions for either removing the sacrificial filaments or casting the surrounding material, and thus could not be accomplished with aqueous-based ECMs or in the presence of living cells.

Here, we describe a biocompatible sacrificial material—a simple glass made from mixtures of inexpensive and readily available carbohydrates—and a means to 3D print the material to facilitate the rapid casting of patterned vascular networks in engineered tissues. This carbohydrate glass formulation was developed specifically to accommodate two seemingly opposing design criteria that we identified for biocompatible 3D sacrificial materials: 1) sufficient mechanical stiffness to physically support its own weight in an open 3D lattice of filaments and 2) the ability to dissolve rapidly and biocompatibly in the presence of living cells.

Carbohydrate glass can be formed by dissolving one or more carbohydrates in water and then boiling of the solvent. Our early experiments were based on a sucrose-glucose mixture developed by the food industry, which showed that while sucrose is unstable in supersaturated solutions, the addition of glucose prevents recrystallization and facilitates the formation of a stable and inexpensive glass [14]. This simple mixture was too hygroscopic and soft to handle. During material optimization and screening of potential additives, we found that the addition of starch stiffened the base material, but it imparted inferior optical clarity and therefore limited potential use with matrices that are commonly crosslinked by photochemical reactions [15, 16]. In contrast, the addition of glycerol preserved clarity but rendered filaments mechanically unstable at room temperature. Ultimately, we further reinforced the glass and improved its temperature stability by incorporating dextrans. Uniaxial compression testing confirmed that the carbohydrate glass is mechanically stiff and brittle at room temperature (Figure 1a). The optical transparency of the glass indicated compatibility with photopolymerization wavelengths in the ultraviolet, visible, and near-infrared ranges, making it unlikely that the glass would leave shadowing artifacts in photoactive scaffolds (Figure 1b).

Multiscale vascular networks are comprised of a range of diameters of vessels and their interconnections. Thermal extrusion and fiber drawing with a 3D printer—a programmable Cartesian coordinate positioning system—provided an effective route to the fabrication of filamentous carbohydrate glass lattices. By varying only the translational velocity of the extrusion nozzle, while holding constant the nozzle diameter and the extrusion flow rate parameters, extruded filament diameters tracked the governing equation:

$$D(v)=\frac{\mathrm{A}}{\sqrt{v}} \quad (1)$$

where $D(v)$ is the resultant filament diameter, A is a constant that incorporates the extrusion nozzle diameter and extrusion flow rate, and $v$ is the velocity of the extrusion nozzle (Figure 1c). This relationship derives from existing models of glass fiber drawing [17] and allowed the generation of carbohydrate glass lattices in predefined, multiscale, and reproducible patterns (Figure 1d–h). Moreover, controlling the temperature of the assembly platform facilitated the formation of smooth melt fusions at filament intersections (Figure 1e).

We next sought to use these lattices as a sacrificial element for creating fluidic channels within monolithic cellularized tissue constructs (Figure 2a). In our strategy, a suspension of cells in ECM prepolymer is poured to encapsulate the lattice. After crosslinking the ECM, the glass filaments are dissolved to form vessels while their interfilament fusions become intervessel junctions (Figure 2b–c). To prevent disruption of ECM crosslinking and to avoid the potential for osmotic damage to encapsulated cells due to carbohydrate dissolution, we coated the carbohydrate glass lattice with a thin layer of poly(D-lactide-co-glycolide) (PDLGA) prior to casting ECM. This coating allowed the dissolved carbohydrates to be owed out of the formed channels instead of through the bulk of the engineered construct (Figure 2b and **Supplementary Movie 1**). Importantly, the coating did not inhibit the ability of the network to support convective and diffusive transport into the bulk gel (Figure 2c). Additionally, we observed that, after sacrifice, the glass interfilament fusions left behind smooth elliptical intervessel junctions that supported fluidic connection between adjoining vascular channels.

To demonstrate the flexibility and generality of this approach, we patterned vascular channels in the presence of living cells in a wide range of natural and synthetic ECM materials (Figure 2d). The time required for encapsulating cells and lattices in ECM prepolymer, ECM crosslinking, and glass dissolution is on the order of minutes. Importantly, we chose ECM materials which varied not only in their bulk material properties but also in their means of crosslinking. Indeed, the approach generated channels without the need to modify handling of aqueous cellularized gels formed by chain entanglements (cooling of agarose), ionic interactions (calcium-polymerized alginate), photopolymerization (synthetic PEG-based hydrogels, [18]), enzymatic activity (thrombin-polymerized fibrin), and protein precipitation (warming of Matrigel). As predicted from characterization of the optical transparency of the carbohydrate glass, photopolymerized gels exhibited no visible shadowing artifacts due to light absorption by the patterned glass lattice. To our knowledge, no other channel-forming technique is compatible with such a wide range of ECM materials. The approach also appears to have no negative effects on cells. Encapsulated cells survived,

spread, and migrated in channeled scaffolds at levels not different from non-channeled control gels, demonstrating biocompatibility of the entire vessel casting process (Figure 2e). Similar viability was found for human umbilical vein endothelial cells (HUVECs), 10T1/2 cells, human fibroblasts, and human embryonic kidney (HEK) cells (data not shown).

Due to the mechanical rigidity and self-supporting nature of the carbohydrate glass lattice, introducing 3D multilayer architecture into the engineered vasculature requires no additional constraints, time, or steps to the sacrificial process (Supplementary Figure S1a). To demonstrate the compatibility of this vascular casting approach with additional design considerations often important to the engineering of tissues, we fabricated complex cellular and immobilized factor gradients in tissue constructs that also contained our channels (Supplementary Figure S1b). Analysis of these tissue constructs (Supplementary Figure S1c) demonstrated that patterning of cells or immobilized factors within the construct into step, linear, and exponential gradients could be accomplished in a single engineered tissue construct containing perfusable vascular channels. Here, cells were encapsulated along with immobilized fluorescent beads as a model factor but this technology should be readily translated to immobilized gradients of adhesive peptides [19], proteins and growth factors [20–22], or the ECM itself [23, 24]. Together, these results illustrate that the available design parameter space for a tissue construct is, for the first time, unhindered by the inclusion of patterned vascular channels and junctions.

Vascularized solid tissues can be conceptually reduced to a “vascular unit cell” comprised of three key compartments: 1) the vascular lumen which serves as both the source and sink for most soluble factors, 2) endothelial cells lining the vascular wall which regulate mass transport exchange with the interstitium, and 3) cells and matrix residing in the interstitial zone between vascular channels (Figure 3a). Here, we demonstrate control over each of these compartments in engineered tissue constructs. The monolithic nature of the gels (resulting from a single step polymerization) and the lack of architectural seams supported non-leaking perfusion of human blood under positive pressure with either laminar or turbulent pulsatile flow (Figure 3b and **Supplementary Movies 2 and 3**), with smooth interchannel junctions supporting branched fluid flow. Endothelial cells seeded through a single inlet in the network quickly lined the walls of the entire network, including the junctions between vessels of differing diameters (Figure 3c,d). Because this endothelium is formed after forming the tissue, these cells and their seeding are independently introduced from cells encapsulated in the interstitial zone. In co-cultures with 10T1/2 cells in the interstitial space, endothelial cells lining the vascular lumen became surrounded by the 10T1/2 cells and formed single and multicellular sprouts extending from the patterned vasculature into the bulk gel (Figure 3e,f).

Engineered constructs densely populated with cells can develop a necrotic core due to lack of adequate mass transport [1]. Thus, a major functional requirement of such an engineered vasculature is its utility to sustain cellular activity in metabolically demanding settings such as physiologically high cell densities. To facilitate imaging of such a densely populated construct, we generated a single layer of parallel fluidic channels formed within the center of a rectangular construct. As a measure of cellular function and activity, we examined expression of destabilized EGFP from a constitutively expressed lentiviral cassette inserted

into HEK293T cells. Monolithic slab gels uniformly distributed with cells exhibited cellular activity only at the gel perimeter (Figure 4a). In contrast, gels with channels rescued protein expression in the gel core, most dramatically around each perfused channel. This preservation of cell function was perfusion-dependent, as EGFP expression was absent near channels without perfusion (data not shown). We also looked at a broader range of cellular densities in these constructs with a functional enzyme assay of a constitutively secreted Gaussia luciferase reporter. At low cell densities, diffusion alone is able to maintain cellular function in bulk gels (Figure 4b). As nutrient requirements of the tissue construct increased with cell density, Gaussia production began to plateau. This limitation was overcome by convective transport through the channeled scaffold. The maintenance of cellular metabolic activity (Figure 4a) as well as secretion of functional proteins and enzymes (Figure 4b) are important functional outputs for many types of engineered tissues [25], both of which appear to be maintained with our engineered vasculature. Together these results illustrate the capacity of patterned perfusable channel architectures to provide functional mass transport to 3D cell cultures at or near physiologic cell densities.

Although these data demonstrate the utility of the approach in supporting a transformed cell line, primary parenchymal cells that would ultimately be required for clinically implanted engineered tissues often cannot tolerate stresses associated with extended periods of suspension and hypoxia. We therefore engineered perfusable gels containing primary hepatocytes, which are known to be highly sensitive to hypoxia and handling (Figure 4c–d). After 8 days in culture, perfusable tissues exhibited substantially higher albumin secretion and urea synthesis compared to slab gels (gels without channels) of the same volume (Figure 4d). Optical sections of these constructs showed that at high cell concentrations cell survival was most prevalent adjacent to perfused channels and decayed radially, consistent with patterns observed in the dsEGFP-expressing HEK293T cells as well as a 3D finite-element model of nutrient delivery to the entrapped cells (Supplementary Figure S2). Together these results illustrate the utility of this strategy for supporting the function of engineered tissues comprised of even highly sensitive primary cells.

Existing methods to create cell-laden gels containing a microfluidic network have required the delicate process of precise stacking and lamination of individually fabricated layers [6–9]. In this study, we found sacrificial carbohydrate glass lattices to be well-suited for the creation of densely populated tissue constructs with perfusable vascular channels and junctions. A key advantage of our method is that the entire perfusable scaffold is formed as a continuous phase simply by filling the 3D void volume around carbohydrate glass lattices and crosslinking the matrix. Cells are encapsulated in ECM and the resulting tissue construct can be perfused within minutes. We believe the sheer rapidity of this process prevents the formation of a necrotic core for metabolically demanding cells during fabrication. Moreover, the microstructural characteristics of the fluidic network—such as vessel diameter, circularity, surface roughness, and junction architecture—arise from fiber drawing and surface tension rather than photolithography or micromachining. Relying on simple physical principles, rather than on engineering processes, enabled the use of low precision hardware to rapidly and reproducibly generate multiscale microvascular architectures in aqueous-based biomaterial scaffolds containing living cells.

Further, the process separation between the 3D microfabrication of filament networks and the handling of cells and ECM allows for dissemination of the technology to distant research laboratories. To illustrate this feature in the current study, carbohydrate glass lattices were shipped under ambient conditions between laboratories. Primary liver hepatocytes were then encapsulated via standard manual pipetting steps to rapidly create perfusable hepatic tissues or non-perfusable control gels. The ability to access this vascularization strategy without fabricating the networks in-house may facilitate rapid adoption of the technology.

Engineered 3D constructs have gained increased attention as *in vitro* tools for the study of cell-cell and cell-matrix interactions, and are being explored for potential use as experimental models or therapeutic replacements of human tissues. However, with the exception of avascular or thin tissues, it has been difficult to achieve the cellular densities of native tissues (approximately 10–500 million cells per milliliter). The approach described here demonstrates an avenue for building and studying such tissue mimics, in which the vasculature appears not to constrain the design space for the tissue itself, allowing for arbitrary cell types, matrices, and their patterning. Coupled with advances in microfluidic device technologies [26, 27], the controlled architecture of these engineered fluidic networks may also provide a means to directly examine the interplay between mass transport requirements of specific tissues and vascular architecture. Moreover, the facile and highly automated nature of this perfusable tissue fabrication strategy should provide a flexible platform for a wide array of specific applications, and may enable the scaling of densely populated tissue constructs to arbitrary size.

## 1. Methods

### 1.1. Preparation and 3D printing of carbohydrate glass

A mixture of 25 g glucose, 53 g sucrose, 10 g dextran (86 kDa), and 50 mL reverse osmosis water (≥18 MΩ; Millipore) was warmed to 165 °C to remove most of the water and form a liquid glass. The hot mixture was poured into a 50 mL syringe that was maintained at 110 °C. The syringe was mounted on a custom modified RepRap Mendel 3D printer with associated electronics (Gen3, MakerBot; RAMPS + RAMMS, Ultimachine). Custom Python scripts were developed to generate the 3D motion control GCode used to drive the machine via open-source ReplicatorG software. Carbohydrate glass lattices were 3D printed at 110 °C under nitrogen pressure with pneumatic control through a 16-gauge or 18-gauge (1.2 mm or 0.84 mm ID, respectively) steel nozzle, vitrified to 50 °C, and then immersed in a 25 mg/mL solution of poly(D-lactide-co-glycolide) (PDLGA; Purac, Amsterdam) in chloroform for up to 5 min. Glass lattices were encapsulated in ECM along with living cells on the same day the lattices were fabricated, or were stored at 45 °C or in a vacuum chamber until use to protect the hygroscopic carbohydrates from absorbing ambient moisture under atmospheric conditions.

### 1.2. Polymer synthesis and cell and lattice encapsulation

Poly(ethylene glycol) diacrylate (PEGDA, 6 kDa or 35 kDa) and acrylate-PEG-RGDS (4 kDa) were synthesized as previously described [18]. In a typical experiment, a prepolymer mixture containing PEGDA (5, 10, or 20 wt%), acrylate-PEG-RGDS (1 mM), photoinitiator

(Irgacure 2959, Ciba Geigy, 0.05% w/v), and cells of interest (1–40e6 cells/mL) was dispensed into rectangular molds containing suspended carbohydrate glass lattices (500 μL total volume per gel). PEG hydrogels were photopolymerized (Omnicure 2000, 320–500 nm) at 100 mW/cm$^2$ for two repetitions of 30 sec duration (rotating 180° about the y-axis before the second exposure). Fibrin gels (10–40 mg/mL) were created by combining fibrinogen, thrombin and cell suspension in phosphate buffered saline (PBS) and then dispensing this mixture around a carbohydrate glass lattice. Fibrin gels were polymerized for 10 min at 37 °C or for 20 min at room temperature. Matrigel constructs were formed by mixing a cell suspension with Matrigel and then dispensing the mixture around a carbohydrate glass lattice, followed by incubation at 37 °C for 10 min. Alginate gels (2%) were formed by mixing an alginate solution with cell suspension, dispensing the mixture around a carbohydrate glass lattice, then carefully crosslinked with a 50 mg/mL $CaCl_2$ solution for 10 min. Agarose gels (2%) were formed by mixing a low-melt agarose solution with cell suspension, dispensing the mixture around a carbohydrate glass lattice, then placed at 4 °C for 20 min. All crosslinked gels were post-processed identically: after crosslinking they were placed in complete medium to dissolve carbohydrate glass (10 min), followed by exchange with fresh medium and cell culture (static culture or orbital shaking at a rate of 2 Hz). In 800 μm channels (diameter) we measured peak flow rates of 10 μL/sec, corresponding to mean velocities of 5 mm/sec and shear stress of 1 dyn/cm$^2$. These values are comparable to physiologic settings. Gel slabs (without vascular architectures) were created by using identical rectangular molds and identical gel processing steps, but without encapsulating glass lattices. Diffusion studies were conducted with fluorescent Cascade Blue Dextran 10kDa (Invitrogen). Fluorescent beads (Polysciences) were mixed with ECM prepolymer mixtures for matrix immobilization or PBS for bead perfusion studies. Heparanized human blood, whole blood, or packed red blood cells (Interstate Blood Bank) were washed and diluted with PBS before use.

### 1.3. Endothelialization of vascular networks

HUVECs were seeded in the vascular lumen by injecting a HUVEC suspension (35e6 cells/mL) into the vascular architecture approximately 10 minutes after the constructs were fabricated. HUVECs were allowed to attach in static culture for one hour before introducing flow, and they reached confluence within 1 day. Endothelialized gels often contained additional HUVECs (1.5e6/mL) and 10T1/2 cells (1.5e6/mL) encapsulated in the bulk gel, such as the gel shown in Figure 3c–f.

## Online Methods

Additional methods may be found online in Supplementary Information.

## Supplementary Material

Refer to Web version on PubMed Central for supplementary material.

## Acknowledgements

We thank the large number of open source and related projects that critically facilitated this work, including Arduino.cc, RepRap.org, MakerBot.com, Replicat.org, MakerGear.com, Ultimachine.com, Hive76.org, Python.org,

Hugin.SourceForge.net, ImageMagick.org, Blender.org, Enblend.sourceforge.net, NIH ImageJ, and Fiji.sc. We thank Robert J. Vlacich and Christopher D. Thompson for assistance with precision pneumatic extrusion, Aaron Dominguez for assistance with red blood cell isolation, and Yi-Ju Chen for assistance with transduction. This work was supported in part by grants from the US National Institutes of Health (EB00262, EB08396, GM74048), the Penn Center for Engineering Cells and Regeneration, and the American Heart Association-Jon Holden DeHaan Foundation. Individual fellowship support was provided by Ruth L. Kirschstein National Research Service Awards from NIH (J.S.M., HL099031; K.R.S., DK091007), the National Science Foundation IGERT program (M.T.Y., DGE-0221664), and the American Heart Association (X.Y., 10POST4220014).

## References

1. Radisic M, Yang L, Boublik J, Cohen RJ, Langer R, Freed LE, Vunjak-Novakovic G. Medium perfusion enables engineering of compact and contractile cardiac tissue. Am J Physiol Heart Circ Physiol. 2004; 286:H507–H516. [PubMed: 14551059]
2. Langer R, Vacanti JP. Tissue engineering. Science. 1993; 260:920–926. [PubMed: 8493529]
3. Griffith LG, Swartz MA. Capturing complex 3d tissue physiology in vitro. Nat Rev Mol Cell Biol. 2006; 7:211–224. [PubMed: 16496023]
4. Vunjak-Novakovic G, Scadden DT. Biomimetic platforms for human stem cell research. Cell Stem Cell. 2011; 8:252–261. [PubMed: 21362565]
5. Schmidt-Nielsen K. Scaling in biology: the consequences of size. J Exp Zool. 1975; 194:287–307. [PubMed: 811757]
6. Golden AP, Tien J. Fabrication of microfluidic hydrogels using molded gelatin as a sacrificial element. Lab Chip. 2007; 7:720–725. [PubMed: 17538713]
7. Ling Y, Rubin J, Deng Y, Huang C, Demirci U, Karp JM, Khademhosseini A. A cell-laden microfluidic hydrogel. Lab Chip. 2007; 7:756–762. [PubMed: 17538718]
8. Choi NW, Cabodi M, Held B, Gleghorn JP, Bonassar LJ, Stroock AD. Microfluidic scaffolds for tissue engineering. Nature materials. 2007; 6:908–915. [PubMed: 17906630]
9. Cuchiara MP, Allen ACB, Chen TM, Miller JS, West JL. Multilayer microfluidic pegda hydrogels. Biomaterials. 2010; 31:5491–5497. [PubMed: 20447685]
10. Visconti RP, Kasyanov V, Gentile C, Zhang J, Markwald RR, Mironov V. Towards organ printing: engineering an intra-organ branched vascular tree. Expert opinion on biological therapy. 2010; 10:409–420. [PubMed: 20132061]
11. Therriault D, White SR, Lewis JA. Chaotic mixing in three-dimensional microvascular networks fabricated by direct-write assembly. Nature Materials. 2003; 2:265–271. [PubMed: 12690401]
12. Bellan LM, Singh SP, Henderson PW, Porri TJ, Craighead HG, Spector JA. Fabrication of an artificial 3-dimensional vascular network using sacrificial sugar structures. Soft Matter. 2009; 5:1354–1357.
13. Wu W, Hansen CJ, Aragón AM, Geubelle PH, White SR, Lewis JA. Direct-write assembly of biomimetic microvascular networks for efficient fluid transport. Soft Matter. 2010; 6:739–742.
14. Reinheimer MA, Mussati S, Scenna NJ. Influence of product composition and operating conditions on the unsteady behavior of hard candy cooling process. Journal of Food Engineering. 2010; 101:409–416.
15. Lutolf MP, Hubbell JA. Synthetic biomaterials as instructive extracellular microenvironments for morphogenesis in tissue engineering. Nat. Biotechnol. 2005; 23:47–55. [PubMed: 15637621]
16. Tibbitt MW, Anseth KS. Hydrogels as extracellular matrix mimics for 3d cell culture. Biotechnol Bioeng. 2009; 103:655–663. [PubMed: 19472329]
17. Heiber J, Clemens F, Graule T, Hülsenberg D. Thermoplastic extrusion to highly-loaded thin green fibres containing pb(zr,ti)o3. Adv. Eng. Mater. 2005; 7:404–408.
18. Miller JS, Shen CJ, Legant WR, Baranski JD, Blakely BL, Chen CS. Bioactive hydrogels made from step-growth derived peg-peptide macromers. Biomaterials. 2010; 31:3736–3743. [PubMed: 20138664]
19. Moon JJ, Hahn MS, Kim I, Nsiah BA, West JL. Micropatterning of poly(ethylene glycol) diacrylate hydrogels with biomolecules to regulate and guide endothelial morphogenesis. Tissue engineering Part A. 2009; 15:579–585. [PubMed: 18803481]

20. DeLong SA, Moon JJ, West JL. Covalently immobilized gradients of bfgf on hydrogel scaffolds for directed cell migration. Biomaterials. 2005; 26:3227–3234. [PubMed: 15603817]
21. Stefonek TJ, Masters KS. Immobilized gradients of epidermal growth factor promote accelerated and directed keratinocyte migration. Wound repair and regeneration : official publication of the Wound Healing Society [and] the European Tissue Repair Society. 2007; 15:847–855.
22. Leslie-Barbick JE, Moon JJ, West JL. Covalently-immobilized vascular endothelial growth factor promotes endothelial cell tubulogenesis in poly(ethylene glycol) diacrylate hydrogels. Journal of biomaterials science Polymer edition. 2009; 20:1763–1779. [PubMed: 19723440]
23. Sundararaghavan HG, Monteiro GA, Firestein BL, Shreiber DI. Neurite growth in 3d collagen gels with gradients of mechanical properties. Biotechnol Bioeng. 2009; 102:632–643. [PubMed: 18767187]
24. Nemir S, Hayenga H, West J. Pegda hydrogels with patterned elasticity: Novel tools for the study of cell response to substrate rigidity. Biotechnol Bioeng. 2009
25. Tsang VL, Chen AA, Cho LM, Jadin KD, Sah RL, DeLong S, West JL, Bhatia SN. Fabrication of 3d hepatic tissues by additive photopatterning of cellular hydrogels. FASEB J. 2007; 21:790–801. [PubMed: 17197384]
26. Thorsen T, Maerkl SJ, Quake SR. Microfluidic large-scale integration. Science. 2002; 298:580–584. [PubMed: 12351675]
27. Atencia J, Beebe DJ. Controlled microfluidic interfaces. Nature. 2005; 437:648–655. [PubMed: 16193039]

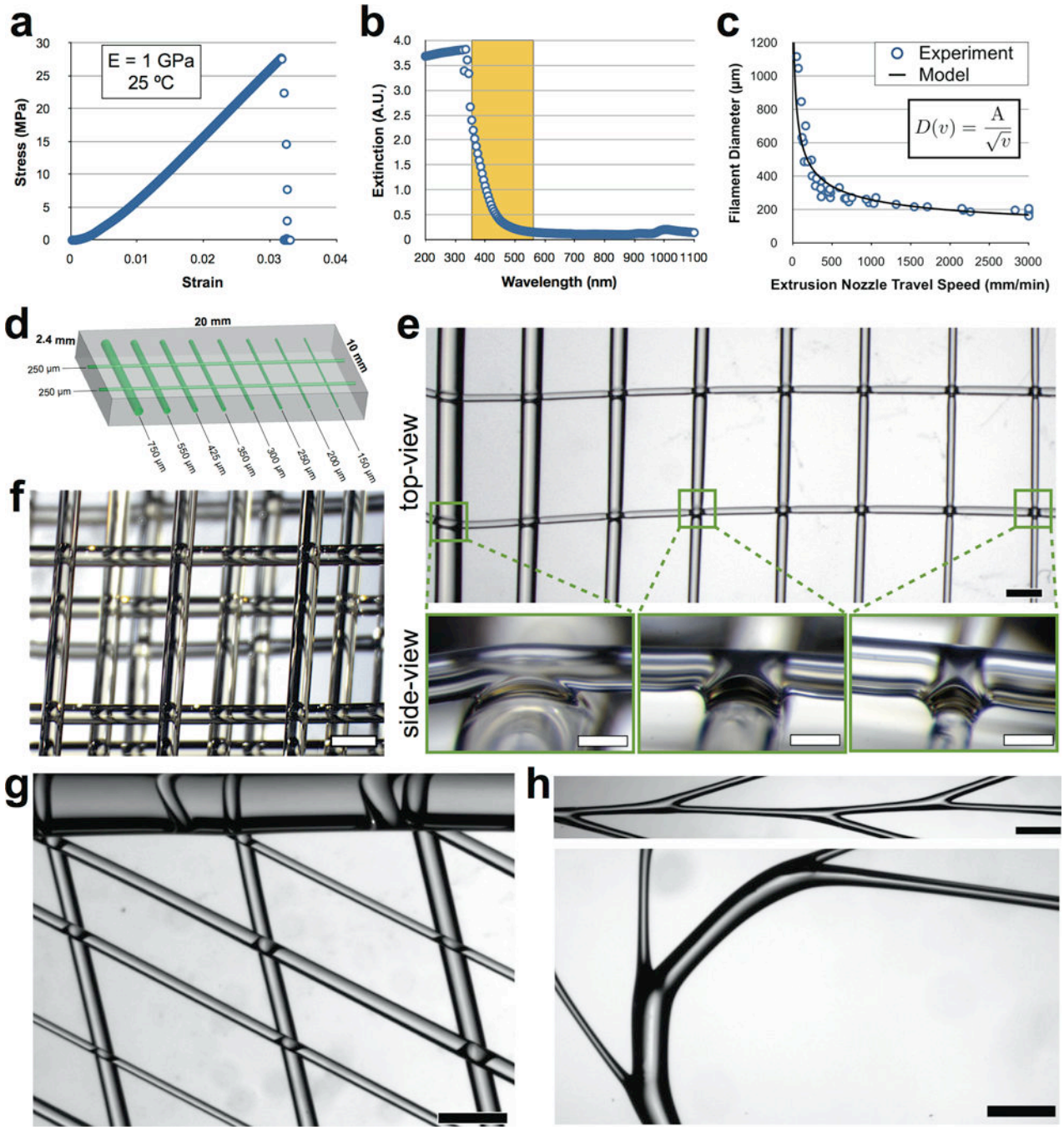


**Figure 1.**

Carbohydrate glass material properties and filament architecture formation. (**a**) Stress-strain curve from uniaxial compression testing indicates the carbohydrate glass is a stiff and brittle material at 25 °C, with Young's modulus = 1 GPa (measured in the linear regime), maximum strength of 28 MPa, maximum strain of 3.25%. (**b**) Optical extinction for a 1 cm sample of carbohydrate glass indicates the material transmits light wavelengths commonly used during biocompatible imaging and photopolymerization (365–550 nm, shaded box). (**c**) During thermal extrusion and 3D printing, filament diameter is controlled by the travel

speed of the extrusion nozzle and follows a simple power law from glass fiber drawing (equation inset). (**d**) Architectural design of a multiscale carbohydrate glass lattice (green). (**e**) Top view of the multiscale architectural design in (d) 3D printed in carbohydrate glass (scale bar = 1 mm). Interfilament melt fusions are magnified and shown in side-view (scale bars = 200 μm). (**f**) Multilayered lattices are fabricated in minutes with precise lateral and axial positioning resolution (scale bar = 1 mm). (**g**) A multiscale architecture showing a single 1 mm filament (top) connected to angled arrays of smaller interconnected filaments (scale bar = 1 mm). (**h**) Serial y-junctions and curved filaments can also be fabricated (scale bars = 1 mm).

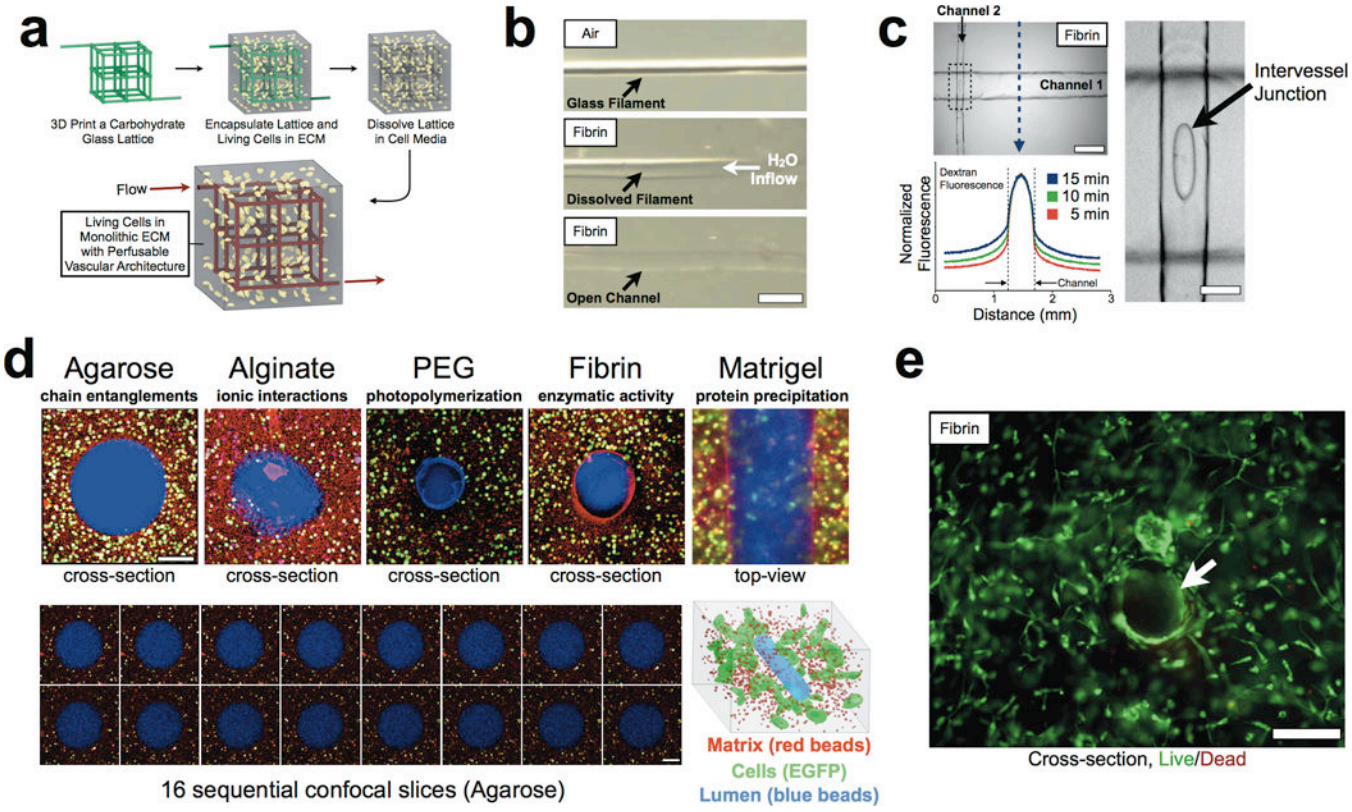


**Figure 2.**

Monolithic tissue construct containing patterned vascular architectures and living cells. (**a**) Schematic overview. An open, interconnected, self-supporting carbohydrate glass lattice is 3D printed to serve as the sacrificial element for the casting of vascular architectures. The lattice is encapsulated in ECM along with living cells. The lattice is dissolved in minutes in cell media without damage to nearby cells. The process yields a monolithic tissue construct with a vascular architecture that matches the original lattice. (**b**) A single carbohydrate glass fiber (200 μm in diameter, top) is encapsulated in a fibrin gel. Following ECM crosslinking, the gel and filament are immersed in aqueous solution and the dissolved carbohydrates are flowed out of the resulting channel (middle). Removal of the filament yields an open perfusable channel in the fibrin gel (bottom, scale bar = 500 μm). See **Supplementary Movie 1** for full time course. (**c**) A fibrin gel with patterned interconnected channels of different diameters supports convective and diffusive transport of a fluorescent dextran injected into the channel network (upper left, phase contrast, scale bar = 500 μm). Line plot of normalized fluorescence across the gel and channel (blue arrow) shows a sinusoidal profile in the channel (between dotted black lines) characteristic of a cylinder and temporal diffusion from the channel into the bulk gel. Enlargement of the dotted box region shows an oval intervessel junction between the two perpendicular channels (right, scale bar = 100 μm). (**d**) Cells constitutively expressing EGFP were encapsulated (5e6/mL) in a variety of ECM materials then imaged with confocal microscopy to visualize the matrix (red beads), cells (10T1/2, green) and the perfusable vascular lumen (blue beads) shown schematically (**bottom right**). The materials have varied crosslinking mechanisms (annotated above images) but were all able to be patterned with vascular channels. Scale bars = 200 μm. (**e**)

Representative cross-section image of unlabeled HUVEC (1e6/mL) and 10T1/2 (1e6/mL) co-cultures (not expressing EGFP) encapsulated uniformly in the interstitial space of fibrin gel (10 mg/mL) with perfusable networks after two days in culture were stained with a fluorescent Live/Dead assay (green, Calcein AM; red, Ethidium Homodimer). Cells survive and spread near open cylindrical channels (highlighted with white arrow). Scale bar = 200 μm.

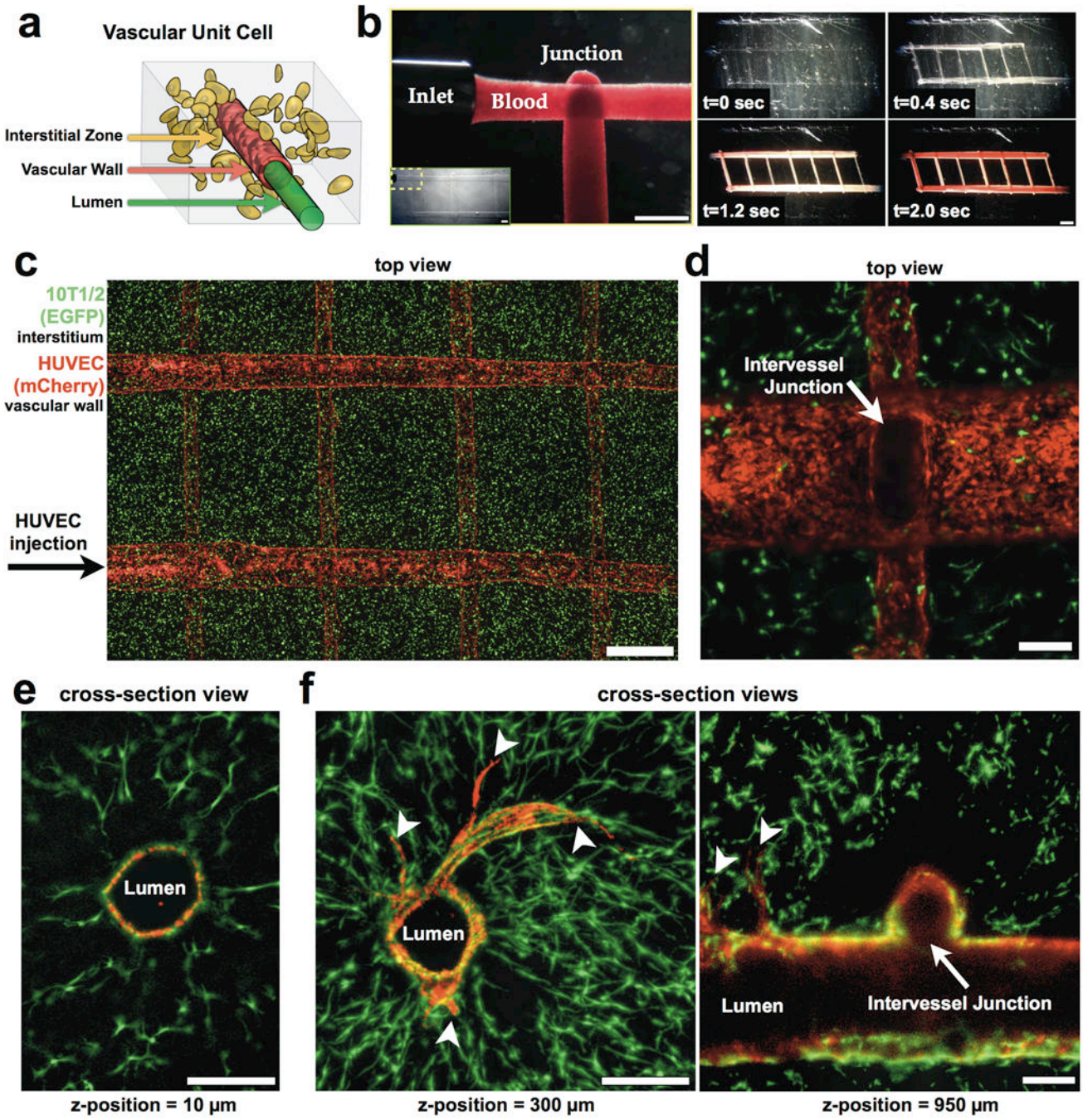


**Figure 3.**

Demonstrated control over the three key compartments of vascularized solid tissues, shown schematically in (**a**) as the "vascular unit cell" comprised of the vascular lumen, endothelial cells lining the vascular wall, and the interstitial zone containing matrix and encapsulated cells. (**b**) Patterned vascular channels support positive pressure and pulsatile flow of human blood with intervessel junctions supporting branched fluid flow (left). Spiral flow patterns (**right**, 0.4 sec) are characteristic of non-laminar flow through cylindrical channels. See **Supplementary Movies 2 and 3**, Scale bars = 1 mm, left; 2 mm, right. (**c**) Control of the

interstitial zone and the lining endothelium of vascularized tissue constructs is demonstrated by encapsulating 10T1/2 cells (1.5e6/mL, constitutively expressing EGFP) in the interstitial space of a fibrin gel (10 mg/mL) followed by seeding of HUVECs (constitutively expressing mCherry) throughout the vascular network via a single lumenal injection (see **Methods**). After one day in culture a confocal z-stack montage demonstrated HUVECs residing in the vascular space with 10T1/2 uniformly distributed throughout the bulk gel. Scale bar = 1 mm. (**d**) A partial z-stack of two intersecting channels demonstrated endothelialization of channel walls and across the intervessel junction, while in the surrounding bulk gel 10T1/2 cells are seen beginning to spread out in 3D. See **Supplementary Movie 4** for the complete 700 μm z-stack from (**d**). (**e**) After 9-days in culture, cross-section imaging of a representative channel (optical thickness and z-position = 10 μm) demonstrated that the endothelial monolayer lining the vascular lumen became surrounded by 10T1/2 cells. Scale bar = 200 μm. (**f**) Endothelial cells formed single and multicellular sprouts (arrowheads) from patterned vasculature as seen in a z-stack (optical thickness = 200 μm) from deeper within the gel (z-position = 300 μm, **left**). Even deeper imaging (z-position = 950 μm, optical thickness = 100 μm, **right**) confirmed that the vascular lumen remained open throughout vessels and intervessel junctions and that endothelial cells also sprouted from larger vessels (arrowheads). See **Supplementary Movie 5** for the complete 1 mm z-stack from (**e,f**).

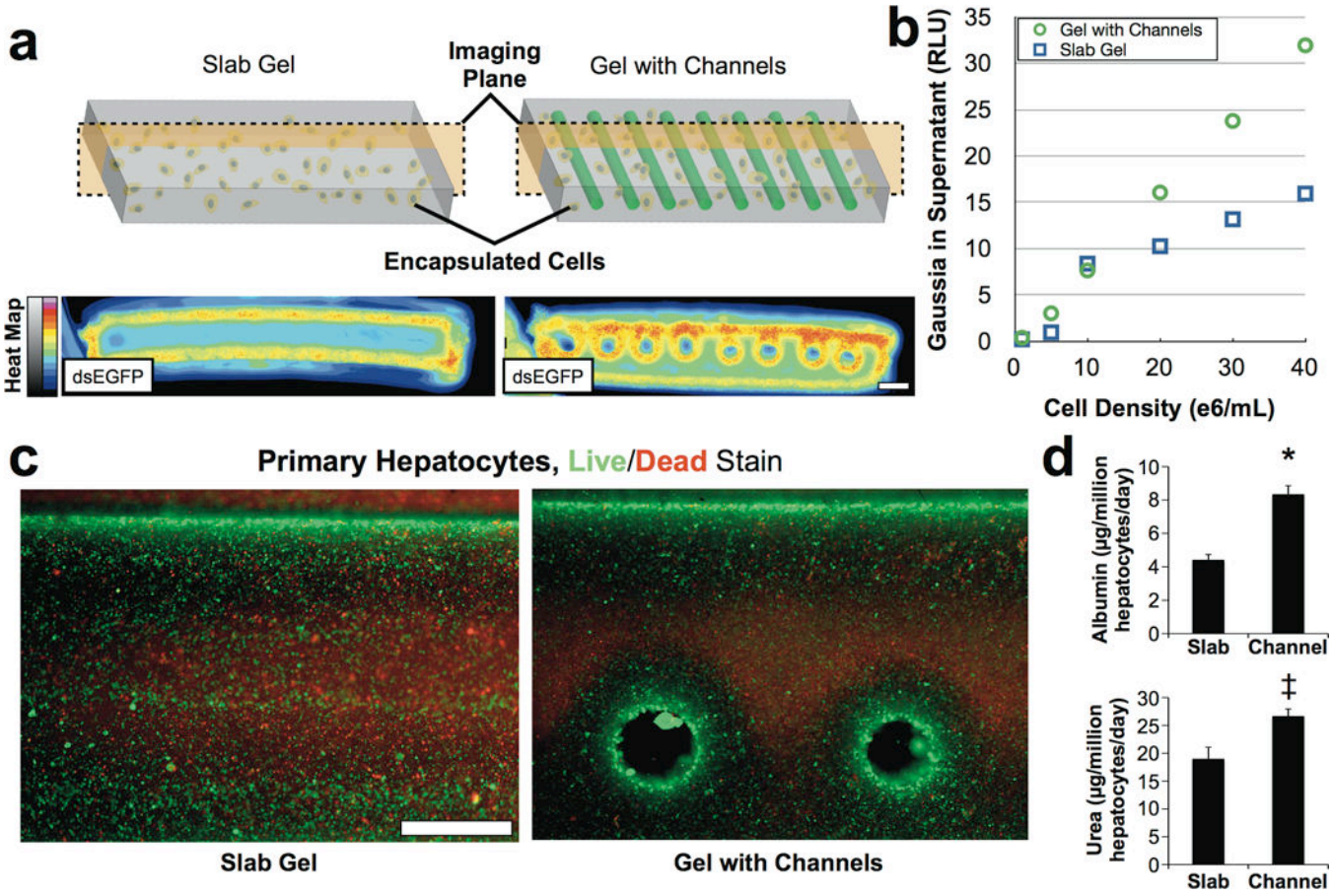


**Figure 4.**

Perfusion channels sustain cellular metabolic function in the core of thick, densely populated tissue constructs. (**a**) Representative cross-section image montages of PEG hydrogels containing 40e6 HEK cells/mL after three days in culture. The intracellular dsEGFP reporter spatially indicates cells are active at the gel slab perimeter and circumferentially around perfusion channels, but not elsewhere in the gel core. Scale bar = 2 mm. (**b**) A functional enzyme assay of secreted Gaussia luciferase from these constructs indicates that the channel architecture preserves cell function even at high cell densities, where function in slab gels quickly falls off. (**c**) Primary rat hepatocytes (24e6 hepatocytes/mL) and stabilizing stromal fibroblasts in agarose gels (slab vs. channeled) after 8 days of culture were stained with a fluorescent Live/Dead assay (green, Calcein AM; red, Ethidium Homodimer). Cells survive at the gel perimeter and near perfused channels, and survival decayed deeper in the gels. Scale bar = 1 mm. (**d**) Assessment of albumin secretion (**top**) and urea synthesis (**bottom**) by primary hepatocytes (16e6/mL) in gels after 8 days of culture demonstrated improved hepatic function in channeled gels compared to slab gels. Error bars represent standard error, p-values for channel versus slab gel comparisons: * < 0.0051; ‡ < 0.045.